AIAA JOURNAL
Vol. 33, No. 12, December 1995

Buckling Analysis of General Triangular Anisotropic Plates Using Polynomials

Navin Jaunky* and Norman F. Knight Jr.†
Old Dominion University, Norfolk, Virginia 23529-0247
and
Damodar R. Ambur‡
NASA Langley Research Center, Hampton, Virginia 23681-0001

The problem of buckling of general triangular anisotropic plates with different boundary conditions subjected to combined in-plane loads is considered. Solutions for plate buckling are obtained by using a Rayleigh–Ritz method combined with a variational formulation. The Ritz functions consist of polynomials that include circulation functions that are used to impose various boundary conditions. Both classical laminated-plate theory and first-order shear-deformation theory are used. Numerical buckling results obtained for isotropic and anisotropic triangular plates are compared with results from existing series solutions.

Nomenclature

A	= area of triangle
b	= height of triangle; see Fig. 3
D_i	= ith displacement component
$\mathbf{J}$	= Jacobian matrix, Eq. (2)
K	= buckling coefficient, Eq. (5)
t	= plate thickness
Γ_i	= circulation function, Eq. (3)
λ_{cr}	= critical eigenvalue
ξ, η, ρ	= area coordinates, Fig. 2

Introduction

THE use of composite materials for aircraft primary structures can result in significant improvements in aircraft performance and structural cost. Such applications of composite materials are expected to result in a 30–40% weight savings and a 10–30% cost reduction compared to conventional metallic structures. Realization of these goals requires the integration of innovative structural concepts, high-performance composite materials and low-cost manufacturing processes. Continuous-filament, grid-stiffened structures that can be manufactured by automated processes to produce wing and fuselage structures have the potential to satisfy these requirements. The stiffener pattern and, hence, the geometry of the skin segments for these structures is primarily determined by the combination of applied in-plane normal and shear loads. Triangular-shaped skin segments result in diagonally stiffened plates. For the case of a panel between frames and stringers of a fuselage section with diagonal stiffeners and a combination of axial and transverse stiffeners, the skin segments have a triangular geometry as shown in Fig. 1. Anisotropic triangular plates result when exploiting structural tailoring characteristics of composite materials.[1] For these applications, stiffener stiffnesses determine the type of boundary conditions imposed along the edges of structural skin segments. Therefore, an analysis method for moderately thick composite plates should be general enough to include different boundary conditions, combined in-plane loading conditions, an arbitrary triangular geometry, and anisotropic material properties. An analytical tool with these capabilities is needed for the preliminary design of stiffened structures.[2,3]

A review of the existing literature indicates that the problem of buckling and vibration of triangular plates has been addressed mostly for isotropic plates. A buckling solution for simply supported equilateral triangular isotropic plates was presented in 1933 by Woinowsky-Krieger as seen in Ref. 4 and in 1957 by Taylor.[5] The stability of simply supported right-angled isosceles triangular isotropic plates subjected to in-plane shear loads was presented in 1951 by Klitcheiff.[6] In 1953, Wittrick[7] improved Klitcheiff's solution to include combined in-plane normal loads and different boundary conditions. Pan[8] obtained the buckling solution for a simply supported 30–60–90 deg triangular isotropic plate subjected to compression in 1956. This problem was treated in 1963 by Reipert.[9] Finally, Valisetty and Reddy[10] presented solutions for simply supported isosceles triangular orthotropic plates subjected to combined in-plane loading in 1985. Their solutions, however, do not satisfy the zero moment conditions at all points along the plate boundaries. The solutions in these references use classical laminated-plate theory (CLPT). The vibration analysis of triangular plates has been studied to a larger extent than the buckling analysis. Vibration of triangular isotropic and orthotropic plates are addressed in Refs. 11–14 using CLPT and in Ref. 15 using a first-order shear-deformation theory (FSDT). The only work dealing with triangular anisotropic plate analysis is reported in Ref. 16, which deals with the free vibration of right-angled triangular plates using CLPT. No work has been reported on the buckling analysis of anisotropic triangular plates with or without transverse shear deformation. The present paper describes analysis methods developed for the buckling of moderately

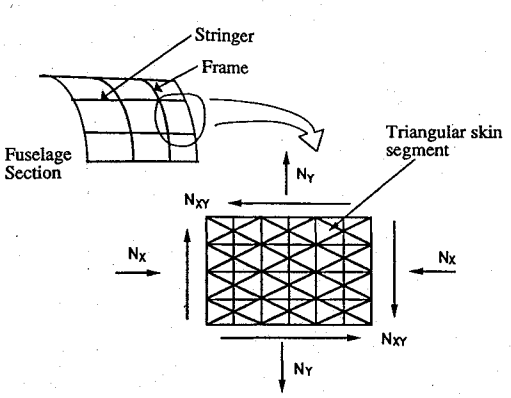

Fig. 1 Fuselage section showing skin segment geometry between stiffeners.

Received Feb. 3, 1995; presented as Paper 95-1456 at the AIAA/ASME/ASCE/AHS/ASC 36th Structures, Structural Dynamics, and Materials Conference, New Orleans, LA, April 10–12, 1995; revision received June 18, 1995; accepted for publication June 20, 1995.

*Graduate Research Assistant, Department of Aerospace Engineering. Student Member AIAA.
†Associate Professor, Department of Aerospace Engineering. Senior Member AIAA.
‡Senior Aerospace Engineer, Structural Mechanics Branch. Associate Fellow AIAA.

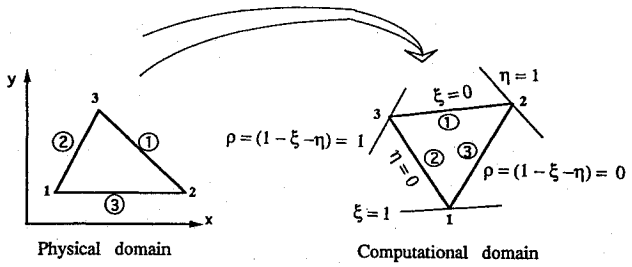

Fig. 2 Physical and computational domains.

thick, general triangular anisotropic plates using FSDT. Analysis results are presented for different triangular geometries, boundary conditions, combined in-plane loading conditions, and material anisotropy. These analysis results are compared with existing results, wherever possible.

Analytical Approach

The formulation of the buckling analysis for a general triangular skin segment (Fig. 2) subjected to combined in-plane loads is done by transforming the physical domain (x, y) to a different computational domain defined in a (ξ, η, ρ) area coordinate system where the displacements and rotations are approximated by selected polynomials. The Jacobian of the transformation is used to relate derivatives in the two domains. Finally, a variational method is used to develop an eigenvalue problem for determining the critical load.

Consider a general triangular plate, shown in Fig. 2, subjected to a state of combined in-plane loads, where the loading and material properties are defined using the coordinate system shown. The physical domain (x, y) is transformed into a computational domain defined by a (ξ, η, ρ) area coordinate system by the following transformation:

$$\begin{aligned} x(\xi, \eta) &= \xi x_1 + \eta x_2 + (1 - \xi - \eta) x_3 \\ y(\xi, \eta) &= \xi y_1 + \eta y_2 + (1 - \xi - \eta) y_3 \end{aligned} \tag{1}$$

where ξ and η are the area coordinates and x_i $(i = 1, 2, 3)$ and y_i $(i = 1, 2, 3)$ are the physical coordinates of the ith corner of the plate. Note that the third area coordinate is expressed in terms of the other or $\rho = (1 - \xi - \eta)$. Transformation of the physical domain to the computational domain is necessary so that boundary conditions can be imposed easily. The Jacobian of the transformation is

$$\mathbf{J} = \begin{bmatrix} \dfrac{\partial x}{\partial \xi} & \dfrac{\partial y}{\partial \xi} \\ \dfrac{\partial x}{\partial \eta} & \dfrac{\partial y}{\partial \eta} \end{bmatrix} \tag{2}$$

According to FSDT, the displacement field has five independent components. The components of the displacement vector are three translations $(D_1, D_2, D_3 = u, v, w)$ and two bending rotations $(D_4, D_5 = \phi_x, \phi_y)$. For the CLPT, the displacement field has three independent components. The components of the displacement vector are three translations $(D_1, D_2, D_3 = u, v, w)$ and the bending rotations are $\partial w/\partial x$ and $\partial w/\partial y$. Each displacement component is approximated independently by different Ritz functions. The approximation for the ith component of the displacement vector is

$$D_i = \sum_{j=1}^{N} a_{ij} d_{ij}$$

where

$$\begin{aligned} d_{ij} &= \Gamma_i(\xi, \eta) \xi^{m_j} \eta^{n_j} \\ \Gamma_i(\xi, \eta) &= \xi^{p_i} \eta^{q_i} (1 - \xi - \eta)^{r_i} \\ m_j, n_j &= (0, 0), (1, 0), (0, 1), (2, 0), (1, 1), (0, 2), \ldots \end{aligned} \tag{3}$$

where d_{ij} represents the jth polynomial term in an N-term approximation for the ith displacement component and a_{ij} are unknown coefficients to be determined. The values of m_j and n_j are used to identify terms in the two-dimensional Pascal's triangle. For example, the pairs of values (m_j, n_j) for all terms in a complete quadratic function would be the six pairs $(j = 1, 2, 3, 4, 5, 6)$ illustrated in Eq. (3). The number of terms N specified for the approximation of each displacement component is selected such that a complete polynomial function in two variables results.

The terms Γ_i in Eq. (3) are used to impose different boundary conditions along plate edges and are referred to as circulation functions because they circulate around the boundary of the plate. Each term Γ_i is the product of three linear functions, and each function is the equation of an edge of the triangle as shown in Fig. 2. The exponents p_i, q_i, and r_i are used to impose different boundary conditions. Only geometric boundary conditions are imposed in this approach; the imposition of boundary conditions when using FSDT is discussed in Ref. 17, and the imposition of boundary conditions when using CLPT is discussed in Ref. 13. Reference 17 also describes the variational statement and the Rayleigh–Ritz method.

Finally, since area coordinates are used, the linear stiffness matrix and geometric stiffness matrix are computed symbolically using the relation

$$\int_A \xi^p \eta^q (1 - \xi - \eta)^r \, dA = 2A \frac{p!\,q!\,r!}{(p + r + q + 2)!} \tag{4}$$

Hence, the transformation from the physical domain to the computational domain also provides an efficient manner to evaluate the integrals appearing in the formulations.

Numerical Results and Discussion

Numerical results are presented for buckling of triangular plates with isotropic and anisotropic material properties. Various geometries, combined in-plane loading conditions, and boundary conditions are considered. Some results obtained using the present method are compared with results from existing series solutions. The effect of transverse-shear deformation on the buckling coefficients of triangular plates is also studied.

Isotropic Triangular Plates

The results for isotropic triangular plates are expressed in terms of a nondimensional buckling coefficient defined as

$$K = \lambda_{cr} b^2 / \pi^2 D_{22} \tag{5}$$

where λ_{cr} is the critical eigenvalue, b the height of the triangle, and D_{22} the transverse plate bending stiffness. The types of triangular plates (see Fig. 3) and boundary conditions considered are 1) simply supported equilateral triangle,[5] 2) right-angled isosceles triangle with simply supported edges,[7] 3) right-angled isosceles triangle with simply supported perpendicular edges and clamped hypotenuse,[7] 4) right-angled isosceles triangle with clamped perpendicular edges and simply supported hypotenuse,[7] and 5) simply supported 30–60–90 deg triangle.[9]

The results obtained using the present analysis are shown in Table 1 for different in-plane loading conditions. The number of terms used in the polynomials for all of these cases is 45 since, as shown in Fig. 4 for the different types of triangular plates subjected to compression $(N_x = N_y = 1)$, the buckling coefficients converged well before 45 terms. These triangular plates have a thickness-to-height ratio (t/b) of 0.0003. Agreement between results obtained using the present method and existing results is very good. Transverse shear effects are negligible for these thin isotropic plates.

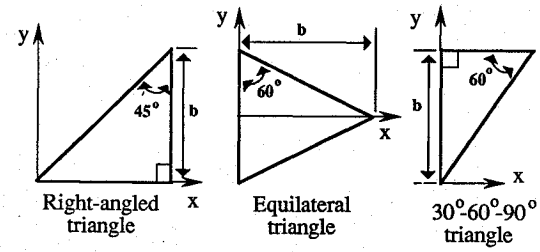

Fig. 3 Triangular geometries.

Table 1 Buckling coefficient K for triangular isotropic plates

Triangle geometry and boundary conditions	Loading	Buckling coefficient		
		Ref. 5 CLPT	Present CLPT	Present FSDT
Equilateral triangle, all edges simply supported	$N_x = N_y = 1$ $N_{xy} = 0$	4.0000	4.0038	4.0038
		Ref. 7 CLPT	Present CLPT	Present FSDT
Right-angled isosceles triangle, all edges simply supported	$N_x = N_y = 0$ $N_{xy} = -1$	11.5500	11.5580	11.5580
	$N_x = N_y = 1$ $N_{xy} = 0$	5.0000	5.0051	5.0051
	$N_x = N_y = 6.29$ $N_{xy} = 11.57$	1.0000	0.9984	0.9984
Right-angled isosceles triangle, perpendicular edges simply supported, hypotenuse clamped	$N_x = N_y = 0$ $N_{xy} = -1$	22.0200	21.9500	21.9500
	$N_x = N_y = 1$ $N_{xy} = 0$	7.8200	7.8171	7.8171
	$N_x = N_y = 8.23$ $N_{xy} = 12.34$	1.0000	0.9898	0.9898
Right-angled isosceles triangle, perpendicular edges clamped, hypotenuse simply supported	$N_x = N_y = 0$ $N_{xy} = -1$	17.1200	16.9390	16.9390
	$N_x = N_y = 1$ $N_{xy} = 0$	9.3500	9.3420	9.3420
	$N_x = N_y = 10.9$ $N_{xy} = 12.34$	1.0000	1.0001	1.0001
		Ref. 9 CLPT	Present CLPT	Present FSDT
30–60–90 deg triangle, all edges simply supported	$N_x = N_y = 1$ $N_{xy} = 0$	9.3300	9.3370	9.3370

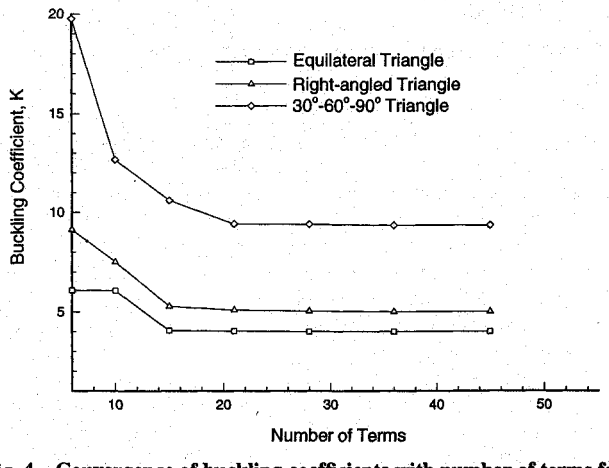

Fig. 4 Convergence of buckling coefficients with number of terms for simply supported triangular plates subjected to compression.

Simply Supported Anisotropic Triangular Plates

Buckling loads for simply supported anisotropic equilateral triangular plates, right-angled isosceles triangular plates and 30–60–90 deg triangular plates are considered in this study. The height of each triangle is 10.0 in. (see Fig. 3). The load cases considered are 1) load case A: $N_x = N_y = 1$, $N_{xy} = -0.5$; 2) load case B: $N_x = N_y = 1$, $N_{xy} = 0.0$; and 3) load case C: $N_x = N_y = 1$, $N_{xy} = 0.5$.

Two laminate stacking sequences are considered herein. Laminates 1 and 2 have ply stacking sequences of $[\pm 45/90/0]_s$ and $[45/90/-45]_s$ with 0.005-in.-thick and 0.007-in.-thick plies, respectively. The nominal ply mechanical properties used are longitudinal modulus = 24.5 Msi; transverse modulus = 1.64 Msi; transverse shear modulus = 0.87 Msi, and major Poisson's ratio = 0.3.

Table 2 Buckling loads results for simply supported triangular anisotropic plates

Triangle geometry	Load case	Laminate 1 N_{cr}, lbs/in. FSDT	Laminate 1 N_{cr}, lbs/in. CLPT	Laminate 2 N_{cr}, lbs/in. FSDT	Laminate 2 N_{cr}, lbs/in. CLPT
30–60–90 deg triangle	A	39.035	39.135	26.795	26.885
	B	45.850	45.999	33.192	33.306
	C	53.960	54.108	42.344	42.495
Right-angled isosceles triangle	A	21.464	21.515	15.574	15.597
	B	25.578	25.642	19.547	19.577
	C	30.567	30.635	25.328	25.372
Equilateral triangle	A	23.702	23.752	20.780	20.789
	B	25.140	25.197	23.626	23.629
	C	25.746	25.804	26.311	26.354

The flexural orthotropy parameter β and the flexural anisotropy parameters γ_b and δ_b are defined as

$$\beta = \frac{(D_{12} + 2D_{66})}{(D_{11}D_{22})^{\frac{1}{2}}}$$
$$\gamma_b = \frac{D_{16}}{\left(D_{11}^3 D_{22}\right)^{\frac{1}{4}}} \tag{6}$$
$$\delta_b = \frac{D_{26}}{\left(D_{22}^3 D_{11}\right)^{\frac{1}{4}}}$$

in Ref. 18. Laminate 1 has flexural anisotropy parameters of 0.208 and 0.182 for γ_b and δ_b, respectively, and a flexural orthotropy parameter β of 1.99. Laminate 2 has flexural anisotropy parameters of 0.528 and 0.376 for γ_b and δ_b, respectively, and a flexural orthotropy parameter β of 1.66. Laminate 1 has a flexural orthotropy parameter of the same order as laminate 2. But laminate 2 has flexural anisotropy parameters higher than laminate 1. Hence, laminate 2 has a higher degree of anisotropy than laminate 1. The converged results obtained using 36 terms (complete eighth-order polynomials in two variables) for each displacement component are shown in Table 2.

For the right-angled isosceles triangular plate and the 30–60–90 deg triangular plate, made of laminate 1, the buckling loads for load case C are approximately 1.4 times the buckling loads for load case A. For the equilateral triangular plate, the buckling load for load case C is approximately 1.1 times the buckling load for load case A. For the right-angled isosceles triangular plate and the 30–60–90 deg triangular plate made of laminate 2, the buckling loads for load case C are approximately 1.6 times the buckling loads for load case A. For the equilateral triangular plate, the buckling load for load case C is approximately 1.3 times the buckling load for load case A. These results indicate that the buckling load is significantly influenced by the symmetry of the triangular plate geometry and material anisotropy when the shear load direction is reversed. The equilateral triangle has three lines of symmetry, the right-angled isosceles triangle has one line of symmetry, and the 30–60–90 deg triangle has no lines of symmetry. The differences between buckling loads obtained using FSDT from those obtained using CLPT are small.

Effect of Transverse-Shear Deformation

The effect of transverse-shear deformation is studied by considering simply supported triangular plates with isotropic and anisotropic material properties and different thickness-to-height ratios (t/b). The triangular plates are subjected to compression loading ($N_x = N_y = 1$). The results for right-angled isosceles and equilateral triangular plates are shown in Table 3 and are expressed in terms of a nondimensional buckling coefficient as defined by Eq. (5). The number of terms used for each displacement component is 45, which coresponds to a complete ninth-order polynomial in two variables.

For both the isotropic triangular plates and anisotropic triangular plates made of laminates 1 and 2, including transverse-shear deformation in the analysis has no significant effect on buckling coefficient results when the (t/b) ratio is increased from 0.001

Table 3 Buckling coefficient K for simply supported triangles with different thickness to height ratios (t/b)

	Right-angled isosceles triangle			Equilateral triangle		
t/b	0.001	0.010	0.100	0.001	0.010	0.100
Isotropic	4.9998	4.9813	4.1014	3.9999	3.9885	3.3864
Laminate 1	5.1528	5.0670	2.9445	4.2697	4.2179	2.6340
Laminate 2	2.6575	2.6311	1.7220	2.6517	2.6263	1.7194

to 0.01. When the (t/b) ratio is increased from 0.01 to 0.1 for the isotropic triangular plates, the buckling coefficient reduces by 18% for the right-angled isosceles triangle and 15% for the equilateral triangle. The corresponding buckling coefficients reductions for laminate 1 are 42 and 38%. For right-angled triangular and equilateral triangular plates made of laminate 2, the reduction is approximately the same at 35%. For typical grid-stiffened composite fuselage structure designs, the (t/b) ratio for triangular plates is greater than 0.025 and, hence, transverse-shear effects need to be included in the analysis.

Concluding Remarks

A buckling analysis method for moderately thick general triangular plates with anisotropic material properties and different boundary conditions subjected to combined in-plane loading has been developed using FSDT. The analysis method is based on a Rayleigh–Ritz method and a variational formulation. Numerical results are obtained for various triangular geometries with isotropic and anisotropic material properties. The direction of the in-plane shear load is studied for different triangular geometries and degrees of material anisotropies. The symmetry of the triangular plate geometry seems to influence the buckling load more than the degree of material anisotropy for the cases considered in this study. The effect of transverse-shear deformation is studied for different triangular geometries, which confirms the importance of including these effects in the buckling analysis of composite plates. The present analytical formulation provides accurate buckling load results for isotropic and anisotropic triangular plates and will be useful in the preliminary design of grid-stiffened structures.

Acknowledgments

The work of the first two authors was supported by NASA Contract NAS1-19858, Task No. 21, and NASA Grant NAG-1-1588, which is gratefully acknowledged.

References

[1]Ambur, D. R., and Rehfield, L. W., "Effect of Stiffness Characteristics on the Response of Composite Grid-Stiffened Structures," *Proceedings of the AIAA/ASME/ASCE/AHS/ASC 32nd Structures, Structural Dynamics, and Materials Conference* (Baltimore, MD), AIAA, Washington, DC, 1991, pp. 1349–1356 (AIAA Paper 91-1087).

[2]Jaunky, N., "Elastic Buckling of Stiffened Composite Curved Panel," M.S. Thesis, Old Dominion Univ., Norfolk, VA, Aug. 1991.

[3]Phillips, J. L., and Gurdal, Z., "Structural Analysis and Optimum Design of Geodesically Stiffened Composite Panels," Center for Composite Materials and Structures, Rept. CCMS-90-05, Virginia Polytechnic Inst. and State Univ., Blacksburg, VA, July 1990.

[4]Timoshenko, S., *Theory of Elastic Stability*, 1st ed., 1936, McGraw–Hill, New York, p. 371.

[5]Taylor, J. L., "Buckling and Vibration of Triangular Flat Plates," *Journal of Royal Aeronautical Society*, Vol. 71, Oct. 1967, pp. 727, 728.

[6]Klitcheiff, J. M., "Buckling of Triangular Plates by Shearing Forces," *Quarterly Journal of Mechanics and Applied Mathematics*, Vol. 4, Pt. 3, 1951, pp. 257–259.

[7]Wittrick, W. H., "Symmetrical Buckling of Right-Angled Isosceles Triangular Plates," *Aeronautical Quarterly*, Vol. 5, Aug. 1953, pp. 131–143.

[8]Pan, L.-C., "Equilibrium Buckling and Vibration of 30–60–90 deg Triangular Plate Simply Supported at the Edges," *Acta Physica Sin.*, Vol. 3, No. 12, 1956, pp. 215–245.

[9]Reipert, Z., "Application of Simple Functional Series to the Solution of Problems Concerning Statics, Stability and Vibration of Plates having Nontypical Forms," *Archiwum Mechaniki Stosowanej*, Vol. 6, No. 15, Warszawa, 1963, pp. 791–814.

[10]Valisetty, R. R., and Reddy, A. D., "Design Data and Buckling of Laminated Composite Triangular Plates," Society of Automotive Engineers, SAE TP Series, SP-623, April 1985, pp. 25–29.

[11]Bucco, D., Mazumdar, J., and Sved, G., "Vibration Analysis of Plates of Arbitrary Shape—A New Approach," *Journal of Sound and Vibration*, Vol. 67, No. 2, 1979, pp. 253–262.

[12]Kim, C. S., and Dickinson, S. M., "The Free Flexural Vibration of Right Triangular Isotropic and Orthotropic Plates," *Journal of Sound and Vibration*, Vol. 141, No. 2, 1990, pp. 291–311.

[13]Singh, B., and Chakraverty, S., "Transverse Vibration of Triangular Plates Using Orthogonal Polynomials in Two Variables," *International Journal of Mechanical Sciences*, Vol. 34, No. 12, 1992, pp. 947–955.

[14]Smith, J. P., "General Plate Stability Using High Order Techniques," *Proceedings of the AIAA/ASME/ASCE/AHS/ASC 33rd Structures, Structural Dynamics, and Materials Conference* (Dallas, TX), AIAA, Washington, DC, 1992, pp. 230–240 (AIAA Paper 92-2283).

[15]Xiang, Y., Liew, K. M., Kitipornchai, S., and Wang, C. M., "Vibration of Triangular Mindlin Plates Subjected to Isotropic In-Plane Stresses," *Journal of Vibration and Acoustics*, Vol. 116, 1994, pp. 61–66.

[16]Liew, K. M., Lam, K. Y., and Chow, S. T., "Study on Flexural Vibration of Triangular Composite Plates Influenced by Fibre Orientation," *Composite Structures*, Vol. 13, 1989, pp. 123–132.

[17]Jaunky, N., Knight, N. F., and Ambur, D. R., "Buckling of Arbitrary Quadrilateral Anisotropic Plate," *AIAA Journal*, Vol. 33, No. 5, 1995, pp. 938–944.

[18]Nemeth, M. P., "Nondimensional Parameters and Equations for Buckling of Anisotropic Shallow Shells," *Journal of Applied Mechanics*, Vol. 61, Sept. 1994, pp. 664–669.